

# Application of the Fenton-like agent based on magnetic iron and manganese oxide in the degradation process of paracetamol in water

Ha Nguyen Manh<sup>1\*</sup>, Long Ha Phuong<sup>1</sup>, Dat Tran Phuc<sup>1</sup>, Huong Tran Thi<sup>2</sup>

<sup>1</sup>Faculty of Chemical Technology, Hanoi University of Industry, Hanoi, 143510, Vietnam

<sup>2</sup>Institute of Materials Science, Vietnam Academy of Science and Technology, Hanoi, 143510, Vietnam

\*Corresponding author: [nmhacnh@gmail.com](mailto:nmhacnh@gmail.com); ORCID ID: [0000-0002-2167-1941](https://orcid.org/0000-0002-2167-1941)

Received: 24 July 2023; revised: 9 September 2023; accepted: 9 October 2023

## ABSTRACT

A Fenton-like catalyst  $\text{MnO}_2\text{-Fe}_3\text{O}_4/\text{SiO}_2$  is synthesized via a two-step approach. The prepared composite has a mesoporous structure and a high surface area of  $190 \text{ m}^2/\text{g}$ . The XRD pattern describes a specific peak of  $\text{Fe}_3\text{O}_4$  magnetite on the baseline of amorphous silica. Furthermore, the FTIR spectra show the height assigned to stretching vibrations of Si-O-Si bonds, Fe-O-Fe connections, and a small peak that matches the Mn-O bonds. SEM images exhibit a porous network structure of the composites with some holes among 30 - 100 nm clusters. The activity of the catalyst is determined in a paracetamol degradation as a Fenton oxidation. The paracetamol removal efficiency is at 85.6% with the optimal conditions as initial pH 3, catalyst dosage of 0.15 g/50 mL and  $\text{H}_2\text{O}_2$  concentration of 1 mL/50 mL. In addition, the catalyst is able to be reused at least five times with a low reduction of the catalytic activity from 85.6% to 80.8%. The experiment results open a direction that has high efficiency in the treatment process of excess paracetamol in pharmacy wastewater.

**Keywords:**  $\text{Fe}_3\text{O}_4$  magnetite, manganese oxide, Fenton process,  $\text{SiO}_2$ , Paracetamol degradation

## INTRODUCTION

The Fenton and the Fenton-like processes are efficient techniques to degrade non-biodegradable organic pollutants [1]. Among Fe-based catalysts, magnetic iron as magnetite ( $\text{Fe}_3\text{O}_4$ ) can be used as a Fenton's reagent, which is environmentally benign, economical, and comparatively anti-toxic. Moreover, this benefit is convenient isolation by a simple magnetic separation [2, 3]. Dispersing the active phase on a support as a heterogeneous system is a possibility to enhance the efficiency and the separated ability [4, 5] due to avoiding the agglomeration, the poison of the active site during the reaction. Among supports such as carbon [3], zeolite [6], diatomite [7], or fly ash [8], amorphous silica from rice husk, a popular agricultural byproduct in Vietnam [8, 9], is an excellent carrier with high surface area, nanoparticle size, and high stability in acid media [8, 10, 11]. Moreover, in a heterogeneous process, the degradation of pollutants in water can occur over a wide pH range [12].

Some promoter phases like  $\text{Mn}^{2+}$ ,  $\text{Co}^{2+}$ ,  $\text{Cu}^{2+}$ ,  $\text{Ag}^+$  [2, 13], etc. can enhance the activity and the stability of the Fenton catalyst. Among them,  $\text{MnO}_2$  exhibited a

good combination with magnetic iron in a Fenton-like process [14, 15]. Due to the exchanged state between redox couple  $\text{Mn}^{4+}/\text{Mn}^{3+}$  during the reaction of  $\text{MnO}_2$  and  $\text{H}_2\text{O}_2$ , the hydroxyl radical ( $\cdot\text{OH}$ ) is formed to reduce organic chemicals, which contributes to more than 95% of the reduction efficiency.

Paracetamol, also known as acetaminophen, is one of the most commonly prescribed drugs used for the reduction of pain, aches, and fevers [16]. However, paracetamol that is excreted through the urine to an aqueous environment has some harmful effects on aquatic life such as genetic code damage, oxidative degradation of lipids, and denaturation of protein in cells, and its toxicity has been well-proven in bacteria, algae, macrophytes, protozoan, and fishes [17, 18]. Recently, there have been several studies about the paracetamol treatment in water by Fenton's process. Some other Fenton's reagent could be used in the process such as  $\text{LaCu}_{1-x}\text{M}_x\text{O}_3$  ( $\text{M}=\text{Mn}, \text{Ti}$ ) composite [1], iron slag (Fe-S) [19], iron oxide (nano)particles [20], etc., which have significant efficiencies. Briefly, Huu Tap Van *et al.* [19] reported that the optimal pH is 3 in paracetamol degradation using iron slag as a catalyst,

and the removal efficiency decreases with the increase of the paracetamol concentration.

This article aims to do an investigation of the paracetamol Fenton degradation, using  $\text{MnO}_2\text{-Fe}_3\text{O}_4$  composite supported on  $\text{SiO}_2$ . The characterization of the catalyst such as XRD, SEM, EDS element distribution, EDS mapping, and FTIR, are recorded. The catalytic activity, stability, and recyclability of the catalyst are investigated through the paracetamol degradation reaction.

## EXPERIMENTAL

**Materials:** All chemicals used in the experiments are analytical grade. Ferrous chloride ( $\text{FeCl}_2 \times 4\text{H}_2\text{O}$ , 99%), ferric chloride ( $\text{FeCl}_3 \times 6\text{H}_2\text{O}$ , 98%), acid hydrochloric (HCl, 36.5%), potassium permanganate ( $\text{KMnO}_4$ , 99%), sodium hydroxide (NaOH, flake 99%), hydrogen peroxide ( $\text{H}_2\text{O}_2$ , 30%), and ammonia solution ( $\text{NH}_4\text{OH}$ , 25-28%) are purchased from Xilong Chemicals Co., Ltd. (Shantou, China). Rice husk that contained 22.5% wt of silica was obtained from a farm in Namdinh province of Vietnam. Paracetamol is purchased from LGC Limited (Germany). Distilled water is obtained in our laboratory from the HAMILTON WSC/4 machine.

**Preparation of the  $\text{MnO}_2\text{-Fe}_3\text{O}_4/\text{SiO}_2$  catalyst:** The  $\text{SiO}_2$  support is prepared from rice husk by a sol-gel method through several steps. Firstly, the rice husk is washed and pretreated with an HCl 1 M solution. Secondly, the clean rice husk is calcined at 700 °C for 2 hours to obtain white ash. Then, use a NaOH 1 M solution to extract silicon oxide from the ash. A colorless solution is obtained from the extraction after filtration, called hydrosol. Next, a silica gel is formed from the hydrosol by using an HCl 1 M solution until pH 5. Last, the gel is aged for 24 h, washed with distilled water, dried at 60 °C for 24 hours, and calcined at 600 °C for 2 h. The obtained product is amorphous silica ( $\text{SiO}_2$ ).

The  $\text{Fe}_3\text{O}_4\text{-MnO}_2/\text{SiO}_2$  catalyst is synthesized through a two-step approach [13]. Firstly, dispersed  $\text{Fe}_3\text{O}_4$  nanoparticles are immobilized on the surface of  $\text{SiO}_2$  through the precipitation process. Briefly, the solutions of precursors iron salts ( $\text{FeCl}_3 \times 6\text{H}_2\text{O}$  and  $\text{FeCl}_2 \times 4\text{H}_2\text{O}$ , molar ratio 1:1) are poured into a silica slurry. The content of the active phase is calculated at about 5 % wt in the catalyst. Then, add a 10% ammonia solution until precipitation (pH = 11). The precipitation is washed, dried, and calcined at 300 °C for 2 hours to form a  $\text{Fe}_3\text{O}_4/\text{SiO}_2$  catalyst. Secondly, the  $\text{MnO}_2$  is coated on the surface of  $\text{Fe}_3\text{O}_4/\text{SiO}_2$  through a hydrothermal method by using  $\text{KMnO}_4$  as a Mn source. The mixture is transferred into a Teflon-lined autoclave and heated to 160 °C for 12 hours. The prepared solid is washed and then dried at 60 °C for 2 hours. The obtained solid is a  $\text{Fe}_3\text{O}_4\text{-MnO}_2/\text{SiO}_2$  catalyst.

**Determination of catalytic activity:** The catalyst activity of  $\text{MnO}_2\text{-Fe}_3\text{O}_4/\text{SiO}_2$  is determined through the paracetamol degradation reaction at room temperature. Briefly, add a certain dosage of catalyst

into the 250 mL beaker containing 50 mL paracetamol solution (20 ppm). Then, stir the mixture for 15 min at 600 rpm. The oxidation reaction begins with the addition of hydrogen peroxide (30%). The temperature is kept at 25 °C. The effects of the reaction time (0-180 min), the catalyst dosage (0.05 to 0.2 g/50 mL), the initial pH (2-8), and the ratio of  $\text{H}_2\text{O}_2$  30% (0.4-1.2 mL/50 mL) on paracetamol removal efficiency are investigated to elucidate the optimal conditions. The initial pH is adjusted by an HCl 0.1 M solution. A UV/Vis spectrophotometer (Thermo Scientific™ GENESYS™ 10S UV-Vis Spectrophotometer) is used to measure the remaining paracetamol concentration in synthetic solutions. The paracetamol removal efficiency (PRE), in percentage, is determined by the decrease in the paracetamol concentration compared to the initial concentration.

The stability and reusability of the catalyst are carried out in the same reaction conditions. Catalysts are washed with distilled water before being used in the next reaction cycle.

**Characterization methods:** A scanning electron microscope (SEM) and the EDS mapping are determined in a Field Emission Scanning Electron S-4800 microscope (Hitachi, Japan). The infrared spectrum of the samples, in the wavelength range of 400-4000  $\text{cm}^{-1}$ , is measured on a Tensor 27-Bruker FTIR spectrometer. XRD patterns of the catalysts are measured on a D8 Advance (Bruker) apparatus at a range from 10° to 70° (scanning step 0.003°, time step 0.8 s, and temperature 25 °C). The Brunauer-Emmett-Teller specific surface area ( $S_{\text{BET}}$ ), adsorption/desorption isotherms, and pore size distribution plot are determined using a specific surface analyzer (Tristar II Plus-Micrometrics).

## RESULTS AND DISCUSSION

### *Physical-chemical characterization of the catalysts:*

Fig. 1 presents the crystal structure of the catalysts via an XRD pattern. It can be observed via a broad band of amorphous silica [21], between  $2\theta$  degrees of 15° and 30° in both patterns. Moreover, the inverse spinel structure of  $\text{Fe}_3\text{O}_4$  magnetite followed six peaks ( $2\theta = 30.2^\circ, 35.6^\circ, 43.3^\circ, 53.7^\circ, 57.5^\circ, 62.9^\circ$ ) in Fig. 1b, which matched as well as (220), (311), (400), (511) and (440) planes in the standard XRD data (JCPDS No. 19-0629) of the cubic spinel structure of magnetite [22]. However, there is no diffraction feature of crystalline  $\text{MnO}_2$  in the XRD pattern. It can be explained by the low crystallinity or amorphous structure of manganese oxide in the composite. Furthermore, because of low content the signal content of  $\text{MnO}_2$  (about 5%, theoretically), the signal could not be strong enough to be against high features and interference from the amorphous silica baseline [22, 23].

The FTIR spectra of the catalyst in Fig. 2 described a vibration of hydroxyl ( $-\text{OH}$ ) groups in the structure of the carrier at the band of 3450  $\text{cm}^{-1}$  and in free water

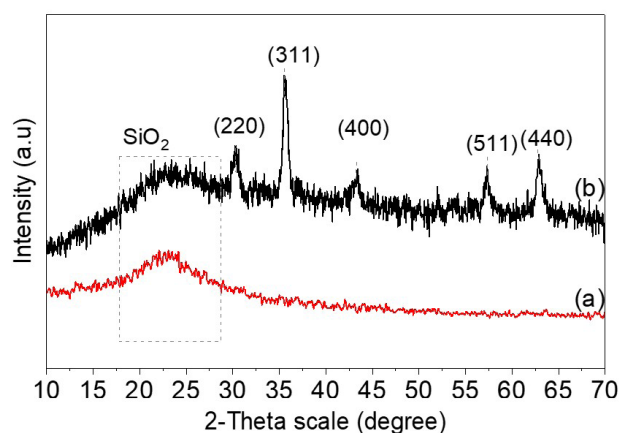


Fig. 1. XRD pattern of SiO<sub>2</sub> support (a) and Fe<sub>3</sub>O<sub>4</sub>-MnO<sub>2</sub>/SiO<sub>2</sub> catalyst (b)

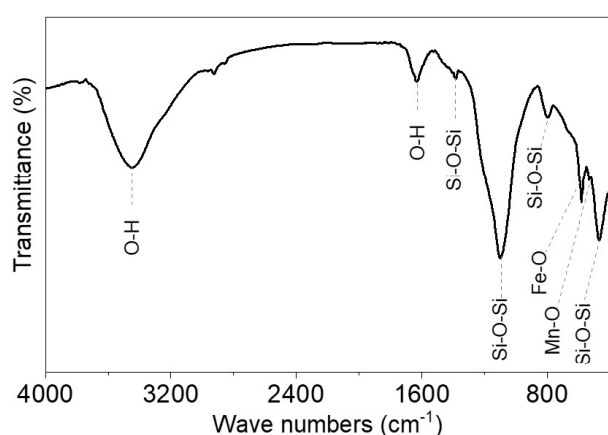


Fig. 2. FTIR spectra of Fe<sub>3</sub>O<sub>4</sub>-MnO<sub>2</sub>/SiO<sub>2</sub> catalyst (c)

on the surface at 1631 cm<sup>-1</sup>. Some peaks that matched the asymmetric stretching, symmetric stretching, and bending modes of the Si-O-Si bond in the support appeared at 1384, 1100, 795, and 468 cm<sup>-1</sup> [24]. Furthermore, a stretching vibration of the Fe-O-Fe bond at about 580 cm<sup>-1</sup> is due to the loading of magnetic iron [13]. On the other hand, an Mn-O vibration in the manganese oxide structure could be ascribed to a small peak at about 532 cm<sup>-1</sup> [13].

The porous properties of MnO<sub>2</sub>-Fe<sub>3</sub>O<sub>4</sub>/SiO<sub>2</sub> catalyst through an N<sub>2</sub> adsorption-desorption isotherm and a plot of pore size distribution are presented in Fig. 3.

It is clear to observe that the catalyst's isotherm is like a type IV curve (IUPAC classification) [25], responding to a mesoporous structure. Moreover, it observed an H3 hysteresis type on the isotherm, as well as the slit pores and laminated structure of the SiO<sub>2</sub> support, which remained after immobilizing Fe<sub>3</sub>O<sub>4</sub> and MnO<sub>2</sub> particles [22]. Thus, it could be the cause of the decrease in the specific surface area from 254.2 m<sup>2</sup>/g to 190.5 m<sup>2</sup>/g after the immobilization. Besides, the plot described that after the addition of active phases, the average pore width of the catalyst is smaller than that of the support, correspondingly, 5.7 nm and 16.9 nm.

Fig. 4 introduced the morphology properties of the

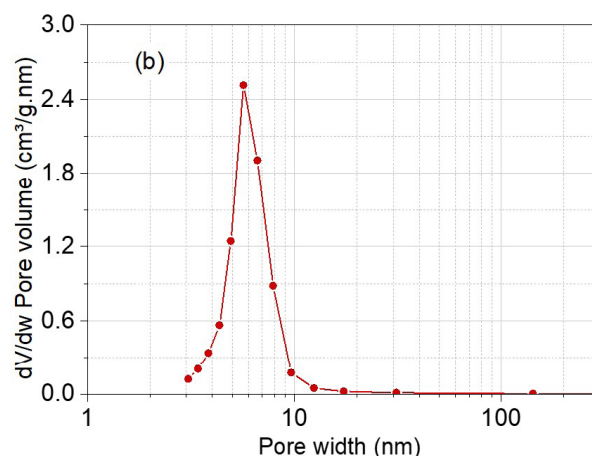
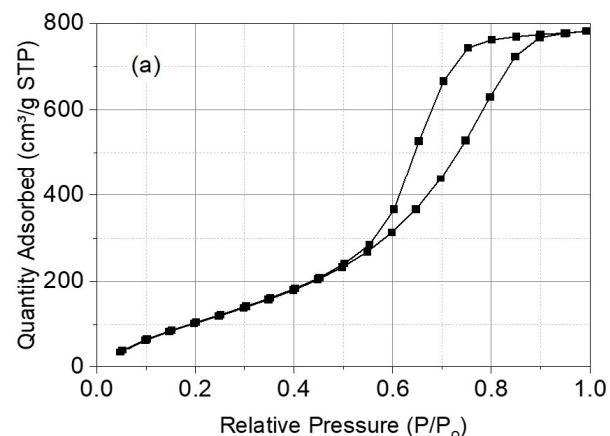


Fig. 3. Adsorption/desorption isotherms (a) and pore size distribution plot (b) of the Fe<sub>3</sub>O<sub>4</sub>-MnO<sub>2</sub>/SiO<sub>2</sub> catalyst

MnO<sub>2</sub>-Fe<sub>3</sub>O<sub>4</sub>/SiO<sub>2</sub> catalysts via SEM images, EDS mapping, and the element distribution. The SEM image presented a porous network structure via a composite structure between some holes and solid clusters with a size of 30 – 100 nm (Fig. 4 a). With lower magnification in Fig. 4 b, the pellets with very different sizes and big holes among them can be observed clearly. They could explain for high surface area and mesoporous structure of the catalyst [21]. Furthermore, the uniform dispersion of Fe<sub>3</sub>O<sub>4</sub> and MnO<sub>2</sub> on the surface of SiO<sub>2</sub> support is provided by the colors corresponding to elements in EDS mapping results from Fig. 4 c to Fig. 4 f, such as green (O), red (Si), sky blue (Mn), and yellow (Fe). In addition, the EDS element contribution in Fig. 4 g showed atomic fractions of 5.08% Fe and 3.02% Mn, as well. Consequently, it can be said that coating magnetic iron and manganese oxide on SiO<sub>2</sub> by a two-step procedure is successful.

**The catalyst performance in the paracetamol degradation:** The MnO<sub>2</sub>-Fe<sub>3</sub>O<sub>4</sub>/SiO<sub>2</sub> catalyst performance in the paracetamol degradation is carried out through the overlay of UV spectra of paracetamol scanned at UV region (210-400 nm). The spectra in Fig. 5a showed one peak at about 258 nm in all curves of reaction time.

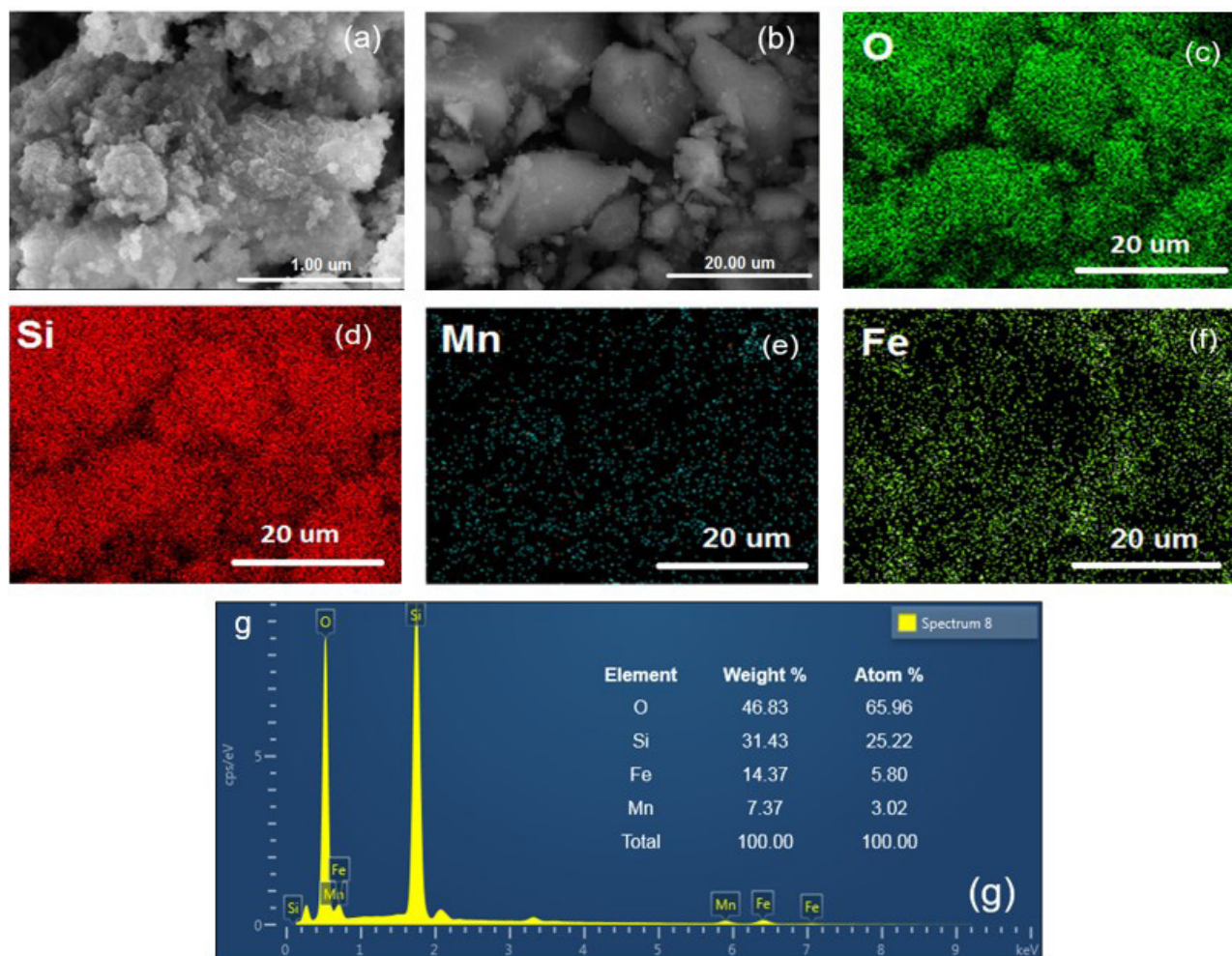
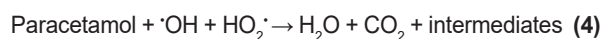
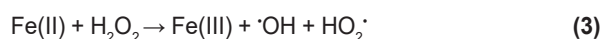
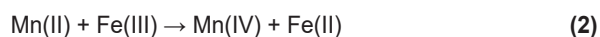
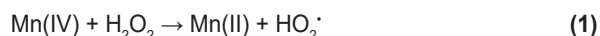


Fig. 4. SEM images (a, b), EDS mapping (c, d, e, f), and element distribution (g) of the catalyst

A probable reaction mechanism of the paracetamol degradation via a Fenton process using the  $\text{MnO}_2\text{-Fe}_3\text{O}_4/\text{SiO}_2$  catalyst [13, 26] can be introduced as follows:



Briefly, superoxide ( $\text{HO}_2^\cdot$ ) and hydroxyl ( $\cdot\text{OH}$ ) radicals are formed in the interaction between  $\text{H}_2\text{O}_2$  and active phase Mn(IV) (in  $\text{MnO}_2$ ), Fe(III) (in  $\text{Fe}_3\text{O}_4$ ) through the reaction (1) to (3). During the process, Mn(IV), and Fe(II) are produced in a redox reaction (2) between the Mn(II) and Fe(III) (in  $\text{Fe}_3\text{O}_4$ ). These reactions happen on the surface of the catalyst. Then, paracetamol can be degraded by the radicals to form water, carbonic gas, and a small number of intermediates such as acetamide, phenol, or alcohols [27], etc.. This is the reason for the decrease in the concentration of paracetamol during the

reaction. The removal efficiency reached 85.6% after 180 minutes of reaction time. It means that the  $\text{MnO}_2\text{-Fe}_3\text{O}_4/\text{SiO}_2$  catalyst exhibited high catalytic activity compared to previous studies [19, 20]. However, other parameters of paracetamol degradation should be investigated to find out the optimal conditions.

The effect of the catalyst dosage on the paracetamol degradation in Fig. 5b shows the PRE increases from 51.2% to 85.6% with the enhancement of the catalyst amount from 0.05 to 0.15 g/50 mL, correspondingly. Because the catalyst is able to enhance the reaction rate, the amount of the oxygenated radicals generated from  $\text{H}_2\text{O}_2$  through reactions (1) and (3) could increase, leading to favor for the decomposition of paracetamol by reaction (4) [7, 19]. However, when the catalyst dosage continues increasing to 0.20 g/50 mL, the PRE only enhances slightly to 87.5%. The reaction appears to reach near the position of the equilibrium which the catalyst has no effect on. Hence, the efficiency will not enhance by the increase of the catalyst dosage. Consequently, the optimal catalyst dosage should be at 0.15 g/50 mL.

Fig. 5c presents the influence of initial pH on the paracetamol removal efficiency. It can be seen that

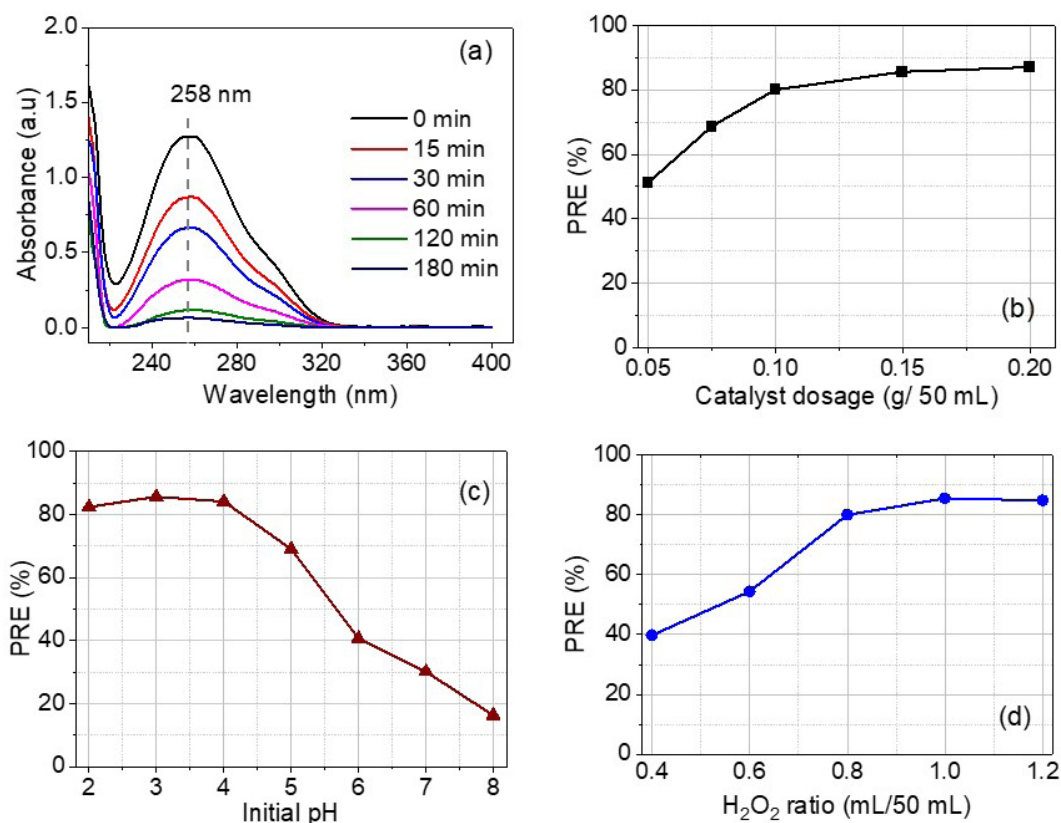


Fig. 5. Effects of some parameters on paracetamol removal efficiency: reaction time (a), catalyst dosage (b), initial pH (c), and H<sub>2</sub>O<sub>2</sub> ratio (d)

a pH greater than 5 is not the optimal medium for the paracetamol oxidation reaction because of the reduction in the production of hydroxyl radicals following the reaction between OH<sup>-</sup> with Fe<sup>2+</sup> and Fe<sup>3+</sup> on the catalyst surface, as well as the degradation of H<sub>2</sub>O<sub>2</sub> to H<sub>2</sub>O and O<sub>2</sub> [23]. Whereas, after 180 min of the reaction time, the PRE is almost similar to pH from 2 to 4 and reached the highest, 85.6%, at pH 3. As a result, the optimal initial pH is 3.

In Fig. 5 d, it can be observed that the enhancement of the H<sub>2</sub>O<sub>2</sub> ratio from 0.4 mL/50 mL to 1.0 mL/50 mL contributes to the increase in the PRE from 40.0% to 85.6%. It can be explained by the direct dependence of the PRE on the number of radicals from reaction (1) to (4) [7, 19]. It means that the paracetamol removal increases with increasing the H<sub>2</sub>O<sub>2</sub> ratio. However, when the H<sub>2</sub>O<sub>2</sub> concentration is too high, the combination of the radicals forming water and gaseous oxygen can happen [23]. It is the cause of the slight reduction of PRE when the H<sub>2</sub>O<sub>2</sub> ratio reaches 1.2 mL/50 mL. Hence, the H<sub>2</sub>O<sub>2</sub> ratio of 1.0 mL/50 mL is likely to be the optimal ratio in the paracetamol degradation using the MnO<sub>2</sub>-Fe<sub>3</sub>O<sub>4</sub>/SiO<sub>2</sub> catalyst.

**The stability and reusability of the catalyst:** Fig. 6 exhibits the stability and reusability of the Fe<sub>3</sub>O<sub>4</sub>-MnO<sub>2</sub>/SiO<sub>2</sub> catalyst in paracetamol degradation.

The experiments show the PRE decreased from 85.6% to 80.8%, after five cycle numbers, and prove the stability of the catalyst for the degradation of paracetamol as

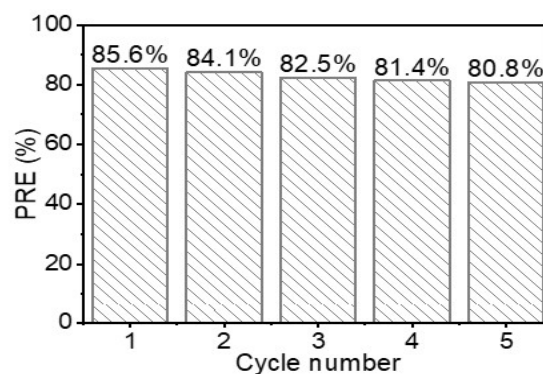


Fig. 6. Investigation of the stability and reusability of the catalyst

the heterogeneous Fenton process. The adsorption of intermediates on the surface of the catalyst can be the cause of the reduction of the PRE in paracetamol degradation [26]. Furthermore, no detectable Fe and Mn ions appear in the liquid, and the atomic fractions of 5.07% Fe and 3.01% Mn in the used catalyst are as well as those in the initial one. Consequently, the MnO<sub>2</sub>-Fe<sub>3</sub>O<sub>4</sub>/SiO<sub>2</sub> nanocomposites have a high stability and reusability in the heterogeneous Fenton process.

## CONCLUSIONS

In conclusion, a two-step procedure successfully synthesizes a Fenton-like agent based on magnetic

iron and manganese oxide on SiO<sub>2</sub> from Vietnam rice husk ash. The characteristic peaks in XRD patterns and FTIR spectra provide the appearance of the metal oxides. The BET method's results introduced a mesoporous structure of the composite. The surface area is 190.5 m<sup>2</sup>/g, lower than the value of the support due to the immobilization. Moreover, EDS mapping showed the even distribution of Fe<sub>3</sub>O<sub>4</sub> and MnO<sub>2</sub> on SiO<sub>2</sub> with atomic fractions of 5.08% Fe and 3.02% Mn. The prepared catalyst has a great exhibition in the degradation of paracetamol. At the optimal condition including pH 3, catalyst dosage of 0.15 g/50 mL, and H<sub>2</sub>O<sub>2</sub> concentration of 1 mL/50 mL, the paracetamol removal efficiency reached around 85.0%. Furthermore, the catalytic stability is good via the decrease in the efficiency from 85.6% to 80.8% after five cycles. Consequently, the MnO<sub>2</sub>-Fe<sub>3</sub>O<sub>4</sub>/SiO<sub>2</sub> has high applicability in the paracetamol treatment in wastewater via a Fenton oxidation process.

## REFERENCES

- Carrasco-Díaz M.R., Castillejos-López E., Cerpán-Naranjo A., and Rojas-Cervantes M.L. (2016) Efficient removal of paracetamol using LaCu<sub>1-x</sub>M<sub>x</sub>O<sub>3</sub> (M = Mn, Ti) perovskites as heterogeneous Fenton-like catalysts. *Chem. Eng. J.*, **304**, 408-418. <https://doi.org/10.1016/j.cej.2016.06.054>
- Xu M., Wu C., and Zhou Y. (2020) Advancements in the Fenton process for wastewater treatment. In: Bustillo-Lecompte C., (Eds), *Advanced Oxidation Processes - Applications, Trends, and Prospects*, IntechOpen. <https://doi.org/10.5772/intechopen.90256>
- Cai X., Zhang Y., Hu H., et al., (2020) Valorization of manganese residue to prepare a highly stable and active Fe<sub>3</sub>O<sub>4</sub>@SiO<sub>2</sub>/starch-derived carbon composite for catalytic degradation of dye waste water. *J. Clean. Prod.*, **258**, 120741. <https://doi.org/10.1016/j.jclepro.2020.120741>
- Pi L., Yang N., Han W., Xiao W., Wang D., et al., (2018) Heterogeneous activation of peroxymonocarbonate by Co-Mn oxides for the efficient degradation of chlorophenols in the presence of a naturally occurring level of bicarbonate. *Chem. Eng. J.*, **334**, 1297-1308. <https://doi.org/10.1016/j.cej.2017.11.006>
- Ouiriemmi I., Karrab A., Oturan N., Pazos M., Rozales E., et al., (2017) Heterogeneous electro-Fenton using natural pyrite as solid catalyst for oxidative degradation of vanillic acid. *J. Electroanal. Chem.*, **797**, 69-77. <https://doi.org/10.1016/j.jelechem.2017.05.028>
- Zhou W.X., Cheng Y., Chen K.Q., Xie G., Wang T., et al., (2020) Thermal conductivity of amorphous materials. *Adv. Funct. Mater.*, **30**(8), 1903829. <https://doi.org/10.1002/adfm.201903829>
- Dai D., Liang H., He D., Potgieter H. and Li M. (2021) Mn-doped Fe<sub>2</sub>O<sub>3</sub>/diatomite granular composite as an efficient Fenton catalyst for rapid degradation of an organic dye in solution. *J. Sol-Gel Sci. Technol.*, **97**, 329-339. <https://doi.org/10.1007/s10971-020-05452-3>
- Vu A.T., Xuan T.N., and Lee C.H., (2019) Preparation of mesoporous Fe<sub>2</sub>O<sub>3</sub>·SiO<sub>2</sub> composite from rice husk as an efficient heterogeneous Fenton-like catalyst for degradation of organic dyes. *J. Water Process Eng.*, **28**, 169-180. <https://doi.org/10.1016/j.jwpe.2019.01.019>
- Ngoc N.N., Thanh L.X., Vinh L.T., and Van Anh. (2018) High-purity amorphous silica from rice husk: Preparation and characterization. *Vietnam J. Chem.*, **56**(6), 730-736. <https://doi.org/10.1002/vjch.201800079>
- Aprilia S., Rosnelly C.M., Zuhra, Fitriani F., Haffiz Akbar E., et al., (2023) Synthesis of amorphous silica from rice husk ash using the sol-gel method: Effect of alkaline and alkaline concentration. *Mater. Today Proc.*, **58**(2), 225-229. <https://doi.org/10.1016/j.matpr.2023.02.403>
- Heo J.N., Do J.Y., Son N., Kim J., Kim Y.S., et al., (2019) Rapid removal of methyl orange by a UV Fenton-like reaction using magnetically recyclable Fe-oxalate complex prepared with rice husk. *J. Ind. Eng. Chem.*, **70**, 372-379. <https://doi.org/10.1016/j.jiec.2018.10.038>
- Jain B., Singh A.K., Kim H., Lichtfouse E. and Sharma V.K. (2018) Treatment of organic pollutants by homogeneous and heterogeneous Fenton reaction processes. *Environ. Chem. Lett.*, **16**(3), 947-967. <https://doi.org/10.1007/s10311-018-0738-3>
- Li Z., Tang X., Liu K., Huang J., Xu Y., et al., (2018) Synthesis of a MnO<sub>2</sub>/Fe<sub>3</sub>O<sub>4</sub>/diatomite nanocomposite as an efficient heterogeneous Fenton-like catalyst for methylene blue degradation. *Beilstein J. Nanotechnol.*, **9**(1), 1940-1950. <https://doi.org/10.3762/bjnano.9.185>
- Zhang W., Yang Z., Wang X., Zhang Y., Wen X., et al., (2006) Large-scale synthesis of β-MnO<sub>2</sub> nanorods and their rapid and efficient catalytic oxidation of methylene blue dye. *Catal. Commun.*, **7**(6), 408-412. <https://doi.org/10.1016/j.catcom.2005.12.008>
- Kim E.J., Oh D., Lee C.S., Gong J., Kim J., et al., (2017) Manganese oxide nanorods as a robust Fenton-like catalyst at neutral pH: Crystal phase-dependent behavior. *Catal. Today*, **282**, 71-76,. <https://doi.org/10.1016/j.cattod.2016.03.034>
- Mahhumane N., Cele L.M., Muzenda C. Nkwachukwu O. V., Koiki B.A., et al., (2022) Enhanced visible light-driven photoelectrocatalytic degradation of paracetamol at a ternary z-Scheme heterojunction of Bi<sub>2</sub>WO<sub>6</sub> with carbon nanoparticles and TiO<sub>2</sub> nanotube arrays electrode. *Nanomaterials*, **12**(14), 2467. <https://doi.org/10.3390/nano12142467>

17. Samira O., Samira A., and Salih L. (2022) Effectiveness of Fenton oxidation for the removal of paracetamol and diclofenac from aqueous medium: effect of operational parameters. *Int. J. Hydrol. Sci. Technol.*, **14**(1), 96. <https://doi.org/10.1504/IJHST.2022.10046090>
18. Pacheco-Álvarez M., Picos Benítez R., Rodríguez-Narváez O.M. Brillas E. and Peralta-Hernández J.M. (2022) A critical review on paracetamol removal from different aqueous matrices by Fenton and Fenton-based processes, and their combined methods. *Chemosphere*, **303**, 134883. <https://doi.org/10.1016/j.chemosphere.2022.134883>
19. Van H.T., Nguyen L.H., Hoang T.K., Nguyen T.T., Tran T.N.H., et al. (2020) Heterogeneous Fenton oxidation of paracetamol in aqueous solution using iron slag as a catalyst: Degradation mechanisms and kinetics: Iron slag-based heterogeneous Fenton degradation of paracetamol. *Environ. Technol. Innov.*, **18**, 100670. <https://doi.org/10.1016/j.eti.2020.100670>
20. Velichkova F., Julcour-Lebigue C., Koumanova B., and Delmas H. (2013) Heterogeneous Fenton oxidation of paracetamol using iron oxide (nano) particles. *J. Environ. Chem. Eng.*, **1**(4), 1214-1222. <https://doi.org/10.1016/j.jece.2013.09.011>
21. Kumar R.S, Vinjamur M., and Mukhopadhyay M.(2013) A simple process to prepare silica aerogel microparticles from Rice husk ash. *Int. J. Chem. Eng. Appl.*, **4**, 321-325. <https://doi.org/10.7763/IJCEA.2013.V4.318>
22. Tang X., Huang J., Liu K., Feng Q., Li Z., et al., (2018) Synthesis of magnetically separable MnO<sub>2</sub>/Fe<sub>3</sub>O<sub>4</sub>/silica nanofiber composite with enhanced Fenton-like catalytic activity for degradation of Acid Red 73. *Surf. Coatings Technol.*, **354**, 18-27. <https://doi.org/10.1016/j.surfcoat.2018.09.011>
23. Sharifi N., Nasiri A., Silva Martínez S., and Amiri H. (2022) Synthesis of Fe<sub>3</sub>O<sub>4</sub>@activated carbon to treat metronidazole effluents by adsorption and heterogeneous Fenton with effluent bioassay. *J. Photochem. Photobiol. A Chem.*, **427**, 113845. <https://doi.org/10.1016/j.jphotochem.2022.113845>
24. Feng Q., Chen K., Ma D., Lin H., Liu Z., et al., (2018) Synthesis of high specific surface area silica aerogel from rice husk ash via ambient pressure drying. *Colloids Surfaces A Physicochem. Eng. Asp.*, **539**, 399-406. <https://doi.org/10.1016/j.colsurfa.2017.12.025>
25. Alothman Z. A. (2012) A review: Fundamental aspects of silicate mesoporous materials. *Materials (Basel)*. **5**(12), 2874-2902. <https://doi.org/10.3390/ma5122874>
26. Dong Fang Z., Zhang K., Liu J., Fan J.Y and Zhao Z.W. (2017) Fenton-like oxidation of azo dye in aqueous solution using magnetic Fe<sub>3</sub>O<sub>4</sub>-MnO<sub>2</sub> nanocomposites as catalysts. *Water Sci. Eng.*, **10**(4), 326-333. <https://doi.org/10.1016/j.wse.2017.10.005>
27. Ghanbari F., Hassani A., Waclawek S., Wang Z., Matyszczyk G., et al. (2021) Insights into paracetamol degradation in aqueous solutions by ultrasound-assisted heterogeneous electro-Fenton process: Key operating parameters, mineralization and toxicity assessment. *Sep. Purif. Technol.*, **266**, 118533. <https://doi.org/10.1016/j.seppur.2021.118533>